ELSEVIER

Earth and Planetary Science Letters 202 (2002) 481–494

EPSL

www.elsevier.com/locate/epsl

Hydrological conditions over the western Mediterranean basin during the deposition of the cold Sapropel 6 (ca. 175 kyr BP)

Edouard Bard [a,b,1,*], Gilles Delaygue [a,c], Frauke Rostek [a,b], Fabrizio Antonioli [d], Sergio Silenzi [d,e], Daniel P. Schrag [b]

[a] *CEREGE, UMR 6635 CNRS and Université Aix–Marseille III, Europole de l'Arbois, 13545 Aix-en-Provence Cedex 4, France*
[b] *Laboratory for Geochemical Oceanography, Department of Earth and Planetary Sciences, Harvard University, 20 Oxford Street, Cambridge, MA 02138, USA*
[c] *LSCE, UMR 1572 CNRS and CEA, Orme des Merisiers, 91191 Gif-sur-Yvette Cedex, France*
[d] *ENEA National Agency for New Technologies, Energy and Environment, via Anguillarese 301, 00060 Roma, Italy*
[e] *ICRAM Central Institute for Marine Research, via Casalotti 300, 00166 Roma, Italy*

Received 8 March 2001; received in revised form 7 June 2002; accepted 18 June 2002

Abstract

A new oxygen isotope record is reported from a stalagmite collected in the Argentarola Cave located on the Tyrrhenian coast of Italy. As shown from observations and numerical modeling of $\delta^{18}O$ in modern precipitation, the recorded $\delta^{18}O$ variability for this zone is dominated by the amount of precipitation (so-called 'amount effect'). The $\delta^{18}O$ profile measured in the stalagmite is characterized by a prominent negative excursion (ca. 2–3‰) between 180 and 170 kyr BP. This paleoclimatic feature is interpreted as being due to a relatively wet period which occurred during the penultimate glacial period, more precisely, during Marine Isotope Stage 6.5. This pluvial phase is shown to correspond chronologically to the deposition of the sapropel event 6 (S6). Although this particular sapropel event occurred during a cold phase, the $\delta^{18}O$ excursion is similar to those corresponding to other sapropels (S4, S3 and S2). The evidence for humid conditions during S6 in the western Mediterranean basin agrees with previous studies based on deep-sea sediment cores. Taken collectively, the data suggest that during sapropel events dilution of ocean surface waters was not restricted to the output of the river Nile but was rather widespread over the entire Mediterranean Sea due to increased rainfall.

Keywords: paleoclimatology; speleothems; sapropels; modeling of oxygen isotopes; Mediterranean Sea

1. Introduction

Marine records of paleoclimate variations of the Mediterranean Sea are characterized by the periodic occurrence of organic-rich layers called sapropels (see the reference graphic in Fig. 1). These events are thought to be due to either increased biological production associated with higher nutrient supply to the euphotic zone, or

* Corresponding author. Tel.: +33-442971561; Fax: +33-442971595.
E-mail address: bard@cerege.fr (E. Bard).

[1] Also at Collège de France.

0012-821X/02/$ – see front matter
PII: S0012-821X(02)00788-4

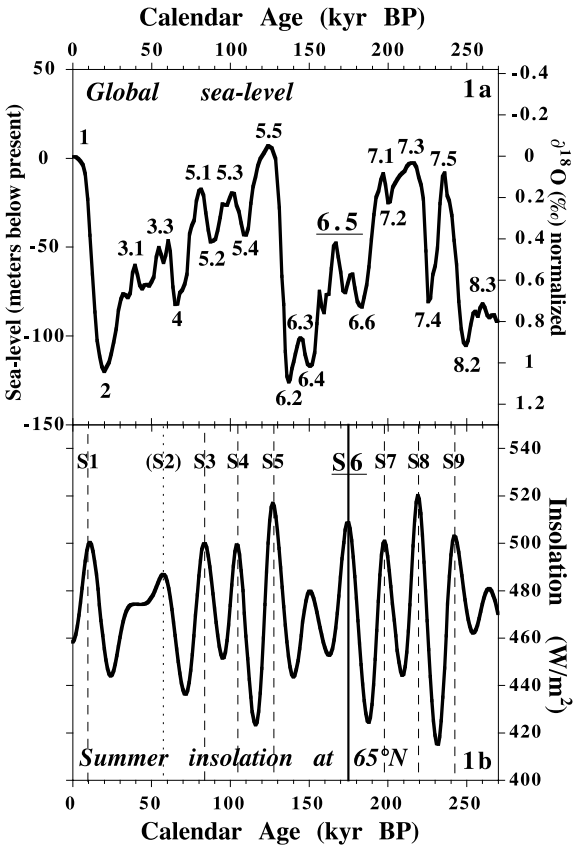

Fig. 1. Diagram summarizing the chronological relationship between the nine most recent sapropel events (S1–S9), the Late Quaternary glaciations (MIS 1–8) and the insolation variations dominated by the 22-kyr orbital precession cycle. (a) Reconstruction of the mean ocean $\delta^{18}O$ from [34] (the right axis gives $\delta^{18}O$ in ‰ relative to zero and the left axis provides a sea level scale). (b) Summer insolation at 65°N from [55] often used to synchronize sapropel events (vertical dashed lines). S2 is placed in parentheses because it is not always present and remains controversial.

increased organic matter preservation in the sediments linked to decreased ventilation and the presence of anoxic deep waters [1]. The increased nutrient supply may have been produced by increased fluxes from rivers, wind-transported dust, nitrogen fixation by marine organisms or through changes in the upwelling of deep and intermediate waters. A few studies have also pointed out the importance of discharge from the Nile [2] although recent work by Sachs and Repeta [3] shows that this river did not supply appreciable quantities of nutrients for phytoplankton growth. The ultimate cause of sapropel deposition is probably linked to drastic changes in the water balance of the Mediterranean Sea, in particular the evaporation–precipitation-runoff budget which controls surface and deep convection [4,5]. In addition, oceanographic modellers have proposed that several circulation patterns for the Mediterranean Sea could explain the formation of sapropels. These range from the anti-estuarine convection system to a hypothetical situation in which there is a reversal towards estuarine type circulation leading to enhanced organic matter preservation [5–7].

A further complication is that several of the proposed mechanisms are not mutually exclusive. For example, because of remineralization, any increase in biological productivity could lead to a decrease in the oxygen content of deep seawater, which in turn would enhance organic matter preservation on the sea floor. A hypothetical circulation reversal leading to low oxygen content in the deep Mediterranean, would have brought up more nutrients to the surface layers, thereby increasing biological productivity and further decreasing deep oxygen concentrations. In addition, most sapropel studies are based on deep-sea sediment proxies that are inherently ambiguous: for example organic matter maxima and redox-sensitive metal enrichments can both arise from the separate or combined effects of increased primary productivity and anoxic conditions.

The identification of the freshwater inputs leading to changes in water density also remains a matter of debate: some authors favor a point-source from the Nile [2] while other invoke multiple sources [8] or a more widespread rainfall increase over the entire Mediterranean basin [5,9].

Deep-sea sediment proxies can be used to identify east–west gradients in salinity in order to separate the different scenarios. The approach is generally based on oxygen isotope records measured in planktonic foraminifera. Therefore the isotope data have to be corrected not only for a global component linked to continental ice-sheets but also for a local imprint due to sea surface temperature (SST) changes [5,8,9]. Most sapropels being deposited during climatic warm phases or even

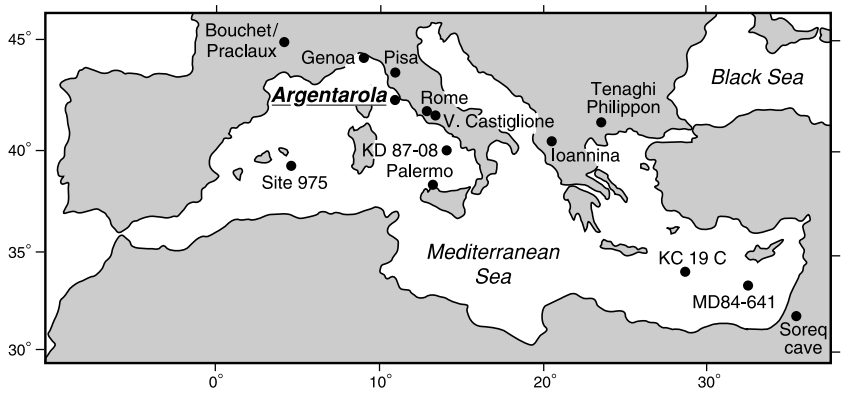

Fig. 2. Location map showing the studied site (Argentarola Island) and the locations mentioned in the discussion and figures (GNIP–IAEA sites, deep-sea sediments cores, terrestrial pollen sequences and Soreq Cave in Israel).

interglacials (Fig. 1), the companion $\delta^{18}O$ decrease can arise from a warming or freshening of the surface. Both enhance water-column stratification through a reduction in surface density. Hence, SST proxies need to be particularly accurate when used for correcting $\delta^{18}O$ records.

A further complication of deep-sea sediments is the presence of diagenetic overprints that can partly erase the sapropel signature, especially its upper part where proxy records are often reoxidized or remobilized [10–13]. This diagenetic bias can affect almost all geochemical proxies measured in the organic and inorganic fractions of the sediment. This is rather unfortunate, since crucial information can be obtained by investigating the details of sapropel events that often exhibit multiple phases separated by the re-establishment of conditions similar to the present day [12,13]. For the most recent S1 event, such a brief interruption has been associated with a cold event at 8.2 kyr BP which could have stimulated the deep convection, thereby recharging the sub-thermocline waters with oxygen [12].

To improve our understanding of the Mediterranean climate during sapropel formation, we selected a completely different type of archive, speleothem calcite, from a site in the Tyrrhenian Sea (western Mediterranean basin). This material is thus very remote from the direct influence of the Nile River discharge. To consider the influence of the freshwater balance without the impact of warming, we studied one of the few sapropels deposited during a cold period. As an additional criterion, the paleoclimatic archive should be datable in order to ensure its correlation with the deep-sea record. The only candidate satisfying the above criteria is the S6 event (Fig. 1) which occurred during the penultimate glacial period, i.e. Marine Isotope Stage (MIS) 6, broadly in phase with substage MIS 6.5 [14,15]. Documenting paleohydrological conditions during S6 will also be useful in discussing the climatic influence of orbital precession at low and mid latitudes under cold conditions [16,17].

2. Site location and modern climatology

The archive selected for stable isotope measurements is a stalagmite collected in a cave located on Argentarola Island off the coast of central Italy, about 100 km north of Rome (42°26′30″N, 11°07′15″E; see Fig. 2). The studied stalagmite is called ASI for Argentarola Stalagmite I [18] and its studied section is shown in Fig. 3. Argentarola Island is very small (200 × 75 m) reaching a maximum elevation of 44 m. Today, there is almost no vegetation and the lack of soil further suggests that such conditions applied during the recent past. The cave located on Argentarola Island is thus an ideal setting for recording the isotopic variations of precipitation free from any continental influences.

Over the last two centuries (1782–1996) the

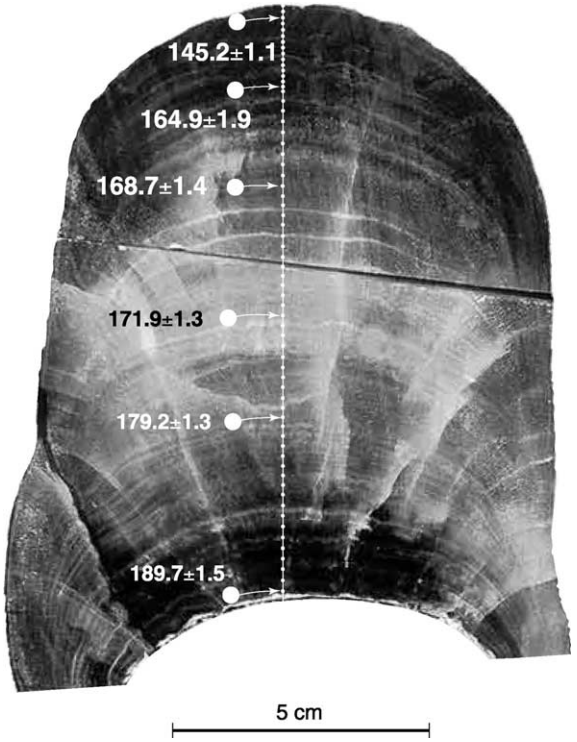

Fig. 3. Photograph of Argentarola Stalagmite I showing the profile sampled for $\delta^{18}O$ analyses and the positions of samples dated by U–Th. This typical stalagmite composed of inorganic calcite was found in situ embedded between two layers of biogenic carbonate. These marine layers were synthesized by marine encrusting worms during interglacial periods when the Argentarola Cave was normally flooded by the Mediterranean Sea [32].

average annual precipitation was 795 ± 176 mm and the mean temperature about 15.8 ± 0.6°C (mean and standard deviation based on the nearby station in Rome [19]). Most precipitation at the site occurs during the winter and is associated with eastward-moving frontal depressions originating from the North Atlantic. For the last two centuries the monthly mean precipitation during winter is 80 ± 30 mm but only 30 ± 20 mm during summer months (mean and standard deviation for December–January–February and June–July–August, respectively).

The General Circulation Model of the NASA Goddard Institute for Space Studies (GISS–GCM) was employed to study rain sources in the Tyrrhenian Sea. We used the outputs from a 6-yr run with interannual variability and with the GISS–GCM at a resolution of $4° \times 5°$ [20]. The mean temperature and precipitation of the grid box corresponding to the Tyrrhenian Sea are 15.8°C and 975 mm/yr, in agreement with observations.

The model indicates a strong local contribution: about 40% of the rainfall water originates from evaporation over the Mediterranean Sea surface. For the studied period (MIS 6) the Mediterranean SSTs were colder than those which prevailed during interglacial periods (e.g. [9,15]). This temperature drop probably decreased somewhat the evaporation over the Mediterranean basin when compared to modern climate. However, a similar cooling affected the Atlantic surface waters during MIS 6.5 (e.g. [21]) and it seems unlikely that the ratio between moisture origins did change dramatically.

3. Oxygen isotopes in modern and past precipitation

Origin of the modern oxygen isotope variability can be studied using data from the Global Network for Isotopes in Precipitation of the International Atomic Energy Agency (GNIP–IAEA) for the three closest available sites: Pisa, Genoa and Palermo [22–24]. Fig. 4a shows the $\delta^{18}O$ of monthly precipitation ($\delta^{18}O_p$) plotted against atmospheric temperature. The plot is characterized by a degree of scatter which is typical of monthly data for mid and low latitudes [22–24]. However, the data for all three sites clearly define a general slope on the order of +0.2‰/°C. For Genoa, the GNIP–IAEA database also enables us to study the interannual variations of $\delta^{18}O_p$ and atmospheric temperature (record equivalent to about 17 yr detrended for seasonal variations following techniques proposed by Rozanski et al. [23]). $\delta^{18}O_p$ and temperature are again positively correlated, with a slope of +0.3‰/°C in broad agreement with values derived from the intra-annual (monthly) data.

The $\delta^{18}O_p$ is also anticorrelated with the amount of precipitation, a behavior usually referred to as the 'amount effect' [25,26]. In the

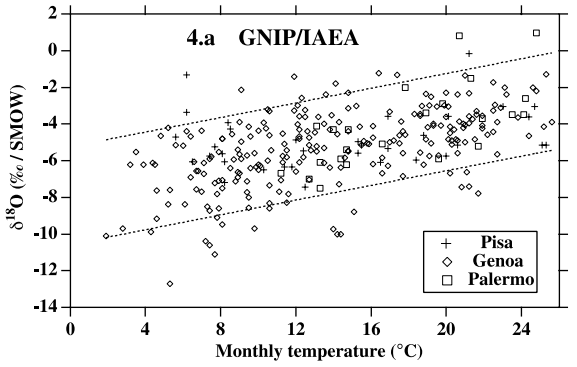

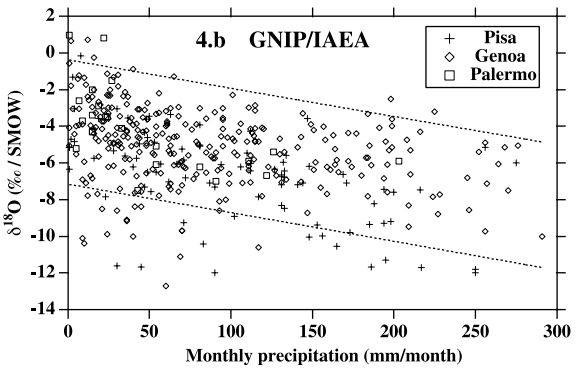

Fig. 4. $\delta^{18}O_p$ of modern precipitation observed at three sites in the GNIP–IAEA database [24] closest to the Argentarola Cave (crosses for Pisa, diamonds for Genoa, squares for Palermo). (a) Monthly mean $\delta^{18}O_p$ plotted vs. monthly mean temperature. The general monthly slope is 0.20 ± 0.02‰/°C ($r = 0.58$, $N = 411$ months). The interannual variations for Genoa give a slope of 0.30 ± 0.04‰/°C ($r = 0.77$, $N = 200$ months). (b) Monthly mean $\delta^{18}O_p$ plotted vs. monthly mean precipitation. The general monthly slope is -1.6 ± 0.2‰ per 100 mm/month ($r = -0.43$, $N = 528$ months; some very rare months with $P > 300$ mm have been excluded). The lines correspond to the prediction envelope at the 95% confidence level.

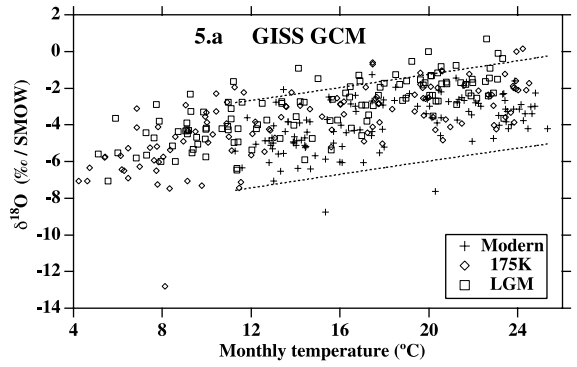

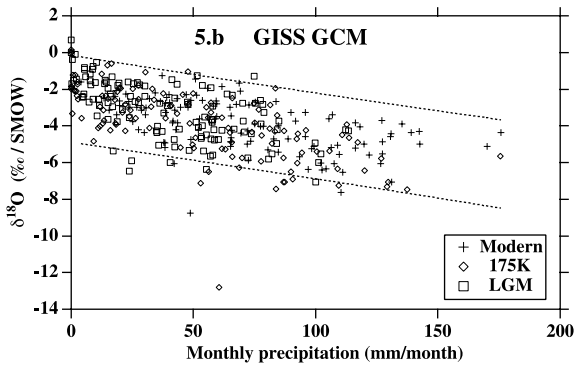

Fig. 5. Estimation of the 'spatial slopes' simulated with the GISS–GCM in the closest fully oceanic Mediterranean box (east box, see text), for modern conditions (crosses), conditions prevailing during the LGM (squares) and MIS 6.5 (called 175K, diamonds). LGM and 175K simulations were run with full glacial boundary conditions, with the respective insolation at 21 and 175 kyr BP. During the first month of the 175K simulation, a short spin-up is responsible for the low isotopic value of −13‰. (a) Monthly mean $\delta^{18}O_p$ plotted vs. monthly mean temperature ($N = 120$ months). The monthly slopes are: 0.18 ± 0.06‰/°C ($r = 0.53$) for the modern climate, 0.26 ± 0.06‰/°C ($r = 0.69$) for the LGM and 0.22 ± 0.04‰/°C ($r = 0.68$) for 175K. (b) Monthly mean $\delta^{18}O_p$ plotted vs. monthly mean precipitation ($N = 120$ months). The monthly slopes are: -2.0 ± 0.6‰ per 100 mm/month ($r = -0.54$) for the modern climate, -3.9 ± 1.0‰ per 100 mm/month ($r = -0.57$) for the LGM and -3.3 ± 0.8‰ per 100 mm/month ($r = -0.66$) for 175K. Note the similarity between modeled values for the three climates, and observed data shown in Fig. 4. The lines correspond to the prediction envelope at the 95% confidence level calculated for modern conditions.

case of the studied zone, the slope of this effect is approximately of −2‰ per 100 mm/month (Fig. 4b). The scatter level is again rather high but this is also a usual feature observed in monthly $\delta^{18}O_p$ data from the GNIP–IAEA database.

To corroborate our study of $\delta^{18}O_p$ composition, we used the GISS–GCM which explicitly includes the hydrological cycle for the different water isotopes [27]. The isotopic GCM was first run for 10 yr under modern boundary conditions with seasonal and interannual variability, in the coarse resolution version (8° × 10°). Each grid box can contain oceanic and continental surfaces. Because of this heterogeneity, and of the coarse resolution, we focused on two grid boxes referred to

as the west and east Mediterranean boxes. The 10-yr average values simulated by the isotopic GCM for temperature (18.1 and 13.7°C, for the east and west box, respectively) and precipitation (850 and 1250 mm/yr, for the east and west box, respectively) are relatively close to mean climatological conditions observed in Rome (15.8°C and 795 mm/yr). Table 1 summarizes all values simulated for the temperature and amount effects for both the east and west boxes. In order to complement Table 1, Fig. 5 shows the outputs from the east box which contains mostly ocean. It is chosen in order to capture the oceanic characteristics of the hydrology over the Tyrrhenian Sea and because precipitation observed at our site (795 mm/yr) is closer to that calculated for the east box (850 mm/yr) than that of the west box (1250 mm/yr). Fig. 5 shows the modeled monthly $\delta^{18}O_p$ plotted against temperature (Fig. 5a) and precipitation (Fig. 5b). Significant correlations are observed (at the 99.5% confidence level) which agree with those based on the GNIP–IAEA data: the temperature effect is about +0.2‰/°C, while the amount effect is approximately −2‰ per 100 mm/month.

The climatic stability of the $\delta^{18}O_p$ sensitivity to temperature and precipitation has been tested by simulating different conditions with this isotopic GCM. We used the outputs of 10-yr simulations, run with seasonal boundary conditions corresponding to the Last Glacial Maximum conditions (called LGM in Table 1 and Fig. 5) and to the same full glacial conditions with the strong insolation characteristic of MIS 6.5 (called 175K in Table 1 and Fig. 5). The paleoclimatic relationships compare well with the present-day ones: the temperature effect is about +0.22‰/°C and the 'amount effect' ranges between −1 and −4‰ per 100 mm/month. If anything, there is a slight tendency for the precipitation sensitivity to increase when climate gets colder: the absolute value for this slope increases from modern to 175K and to LGM climates, for both the east and west Mediterranean boxes (see Table 1).

At this point, it should be emphasized that the studied paleoclimatic archive is a stalagmite composed of inorganic calcite. Precipitation of this mineral is accompanied by a well-known isotopic fractionation of −0.23‰/°C due to the temperature effect [28]. By chance, this thermodynamic fractionation quantitatively compensates for the $\delta^{18}O_p$–temperature dependence observed in the

Table 1
Summary of the relationships between $\delta^{18}O_p$, temperature and precipitation simulated with the GISS–GCM under different climatic boundary conditions ('spatial' relationships for Modern, 175 K and LGM and 'temporal' relationship 175–LGM; see text for details). LGM and 175K simulations were run with full glacial boundary conditions, with the respective insolation at 21 and 175 kyr BP. Values for the slope, 2σ and correlation coefficient (r) are first provided for the west and east box separately, and then for the combined dataset (entitled all). We used monthly averages from the 10 yr of simulation in order to sample the seasonal and interannual variability of each climate. The east box is probably best to represent the climatic conditions over the Tyrrhenian Sea (by contrast with the west box, the east box is close to be fully oceanic and its mean precipitation, 850 mm/yr, agrees well with observations, 795 mm/yr [19]).

	Modern			175 kyr BP			LGM			175 K–LGM		
	west box	east box	all	west box	east box	all	west box	east box	all	west box	east box	all
Temperature effect (‰/°C)	0.31	0.18	0.32	0.17	0.22	0.24	0.22	0.26	0.29	0.17	0.22	0.25
2σ	0.04	0.06	0.04	0.04	0.04	0.04	0.06	0.06	0.04	0.01	0.01	0.004
r	0.83	0.53	0.78	0.55	0.68	0.70	0.53	0.69	0.71	0.59	0.73	0.75
Amount effect (‰/100 mm)	−0.9	−2.0	−2.3	−1.0	−3.3	−2.8	−1.7	−3.9	−3.8	−1.2	−3.4	−3.0
2σ	0.8	0.6	0.6	1.4	0.8	1.0	1.4	1.0	1.0	0.2	0.2	0.2
r	−0.20	−0.54	−0.49	−0.14	−0.66	−0.37	−0.21	−0.57	−0.42	−0.20	−0.67	−0.42

Each box $N = 120$ months, 5000 values; all boxes $N = 240$ months, 10 000 values.

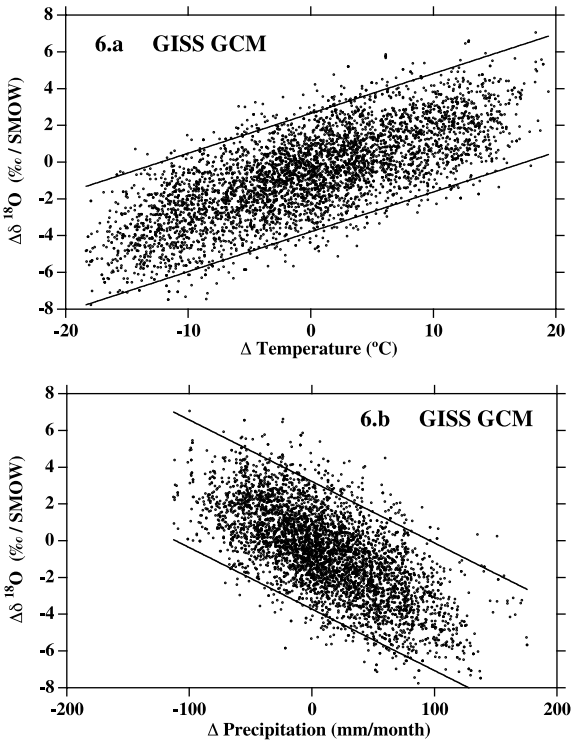

Fig. 6. Estimation of the 'temporal slopes' simulated by the GISS-GCM in the closest fully oceanic Mediterranean box (east box, see text). a/ monthly $\delta^{18}O_p$ and surface temperature, b/ monthly $\delta^{18}O_p$ and precipitation. We applied a Bootstrap statistical technique to the monthly ouputs of both simulations (10 yr), by randomly re-sampling both outputs 5000 times. The correlations between these new samples give an estimation of the temporal slopes: $\Delta\delta^{18}O_p/\Delta T = 0.22$ ‰/°C ($r = 0.73$); $\Delta\delta^{18}O_p/\Delta P = -3.4$ ‰ per 100 mm/month ($r = -0.67$); where Δ stands for a climatic variation. A systematic sampling of the differences ($120 \times 120 = 14400$ values) leads to the same relationships without improving the correlation coefficients. The lines correspond to the prediction envelope at the 95% confidence level.

atmosphere (median of about +0.23 ‰/°C, see discussion above). In other words, the $\delta^{18}O$ measured in the calcite of the Argentarola Cave stalagmite is almost insensitive to temperature change. This is very different from the case of speleothems from higher latitudes which can be sensitive to local temperature because the local slope of the temperature-$\delta^{18}O_p$ is much larger (see [29] for a recent study). By contrast the $\delta^{18}O$ variability in the Argentarola stalagmite is expected to be due to the amount of rainfall and/or isotopic changes at the precipitation source.

To interpret quantitatively the measured isotopic fluctuations in terms of precipitation change, a temporal relationship is needed that is a correlation of the changes between different climates. The studied stalagmite section spans MIS 6 and there is thus a special interest in determining the temporal relationship between full glacial climate (MIS 6.6 and MIS 6.4, see Fig. 1) and milder conditions during MIS 6.5. We estimated such a relationship based on the LGM and 175K 10-yr simulations. Each output of 120 months was randomly resampled 5000 times, assuming that they truly represent the climate variability. Fig. 6 shows the correlations between the 175K–LGM differences from these new datasets. The temporal sensitivity to the temperature for the east Mediterranean box is found to be 0.22 ‰/°C (Fig. 6a) and the temporal 'amount effect' −3.4 ‰ per 100 mm/month (Fig. 6b). Both values are quite close to the observed and modeled spatial relationships (Figs. 4 and 5; Table 1). A systematic sampling of the differences ($120 \times 120 = 14\,400$ values) leads to the same relationships without improving the correlation coefficients.

Masson et al. [17] demonstrated that high insolation can generate increased monsoon activity even with surface glacial conditions. Although it has a coarser resolution (8°×10° vs. 4°×6 for [17]), the isotopic GISS–GCM also simulates an increase of rainfall over the Mediterranean basin for the 175K relative to the LGM conditions. For the east box the model predicts a precipitation difference of about 25%, equivalent to 40–50 mm/month. This increase is much smaller for the west box (5%, not really significant). However, this box is not representative of the Mediterranean Sea as it contains a significant portion of continental surface (see also the discussion above).

4. Oxygen isotopes record and paleoclimatic implications

Carbonate samples were drilled out every 1–2 mm along the central axis of the stalagmite

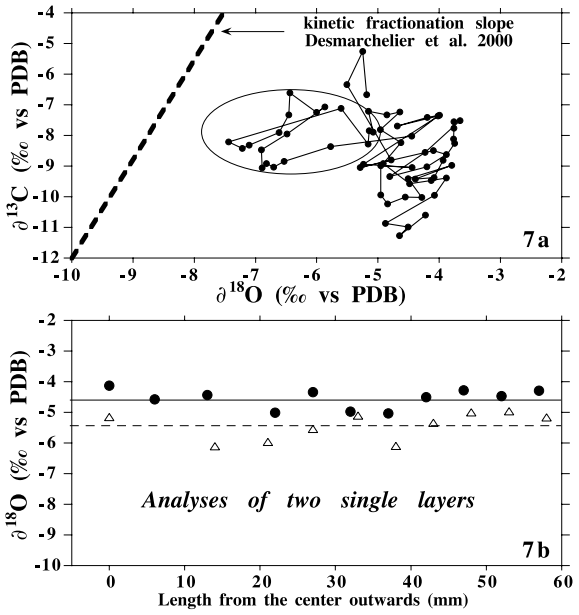

Fig. 7. Tests to check the validity of the $\delta^{18}O$ record [30]. (a) $\delta^{13}C$ vs. $\delta^{18}O$ showing a lack of correlation. The dashed line indicates the kinetic fractionation slope ($\Delta\delta^{13}C/\Delta\delta^{18}O = 3.3$) established by Desmarchelier et al. [31] by measuring stable isotopes in actively growing straw-stalactite tips. Points are connected according to their respective position on the sampling profile. The ellipse underlines the points corresponding to the low $\delta^{18}O$ excursion. (b) $\delta^{18}O$ values measured along two different growth layers (dots and triangles for layers centered respectively at 92 and 106 mm from the top). The lack of a significant $\delta^{18}O$ increase points to the absence of a kinetic isotopic effect. This confirms that the ca. 1‰ shift between the two different layers in (a) corresponds to a genuine thermodynamic isotope fractionation (in other words, the $\delta^{18}O$ record obtained from the sampling profile shown in Fig. 3 would remain unaffected if it had been sampled off the central axis). The residual variability seen in (b) is probably due to the difficulty of sampling along thin single laminae.

ASI (Fig. 3). Stable isotopes measurements were performed at Harvard University with an OPTIMA mass spectrometer. The precision based on replicates of an internal standard is better than 0.06‰. The absence of artifacts linked to kinetic fractionation was checked by means of conventional tests [30]. Indeed, Fig. 7a shows the absence of any specific correlation between $\delta^{18}O$ and $\delta^{13}C$ such as observed by Desmarchelier et al. [31] (see their figure 4). Furthermore, there is no systematic $\delta^{18}O$ increase in synchronous samples taken in two different layers along the side of the stalagmite (Fig. 7b).

The chronology of the 120-mm continuous section (Figs. 3 and 8a) is based on TIMS U–Th ages [32]. Fig. 8a shows the $\delta^{18}O$ time series which falls entirely within MIS 6. The correspondence of this section with the penultimate glacial period is further confirmed by the fact that ASI is today submerged at about 19 m below present mean sea level (MSL). Indeed, calcite precipitation in Argentarola Cave was possible only during extended periods of relatively low sea levels such as during MIS 6 [32].

The $\delta^{18}O$ record is characterized by a marked decrease of 2–3‰ which occurred between 180 and 170 kyr BP. Based on the observed and modeled sensitivity of $\delta^{18}O_p$ to precipitation, we believe that this $\delta^{18}O$ shift is related mainly to a very humid phase. However, the $\delta^{18}O$ lowering between 180–170 kyr BP may also be partly due to $\delta^{18}O$ changes at the sources of precipitation. In fact, Kallel et al. [9] showed that the surface-water $\delta^{18}O$ of the Tyrrhenian Sea was lower by about 1.2‰ at that time due to surface ocean dilution (results based on deep-sea sediment core ED87-08 in Fig. 2). More recently, Emeis et al. [33] evaluated the $\delta^{18}O$ decrease during the ten most recent sapropel events by using alkenone SST and planktonic foraminifera $\delta^{18}O$ from several cores from the eastern and western basins. For S6, these authors observed even larger seawater $\delta^{18}O$ depletions (about −3‰) in both the western and eastern Mediterranean basins. Assuming that the Mediterranean contribution of precipitation remained similar to modern values (ca. 40%, see GCM results described above), a $\delta^{18}O$ decrease ranging between 0.5 and 1.2‰ may thus be attributed to this Mediterranean source effect (40% × 1.2‰ = 0.5‰; 40% × 3‰ = 1.2‰).

Another small source effect must be taken into account because global sea level fluctuated during MIS 6 which led to $\delta^{18}O$ changes of the mean ocean. In fact this global effect is included in the surface $\delta^{18}O$ changes reconstructed for the Mediterranean Sea [9,33], but it must be taken into account for the remaining part of the precipita-

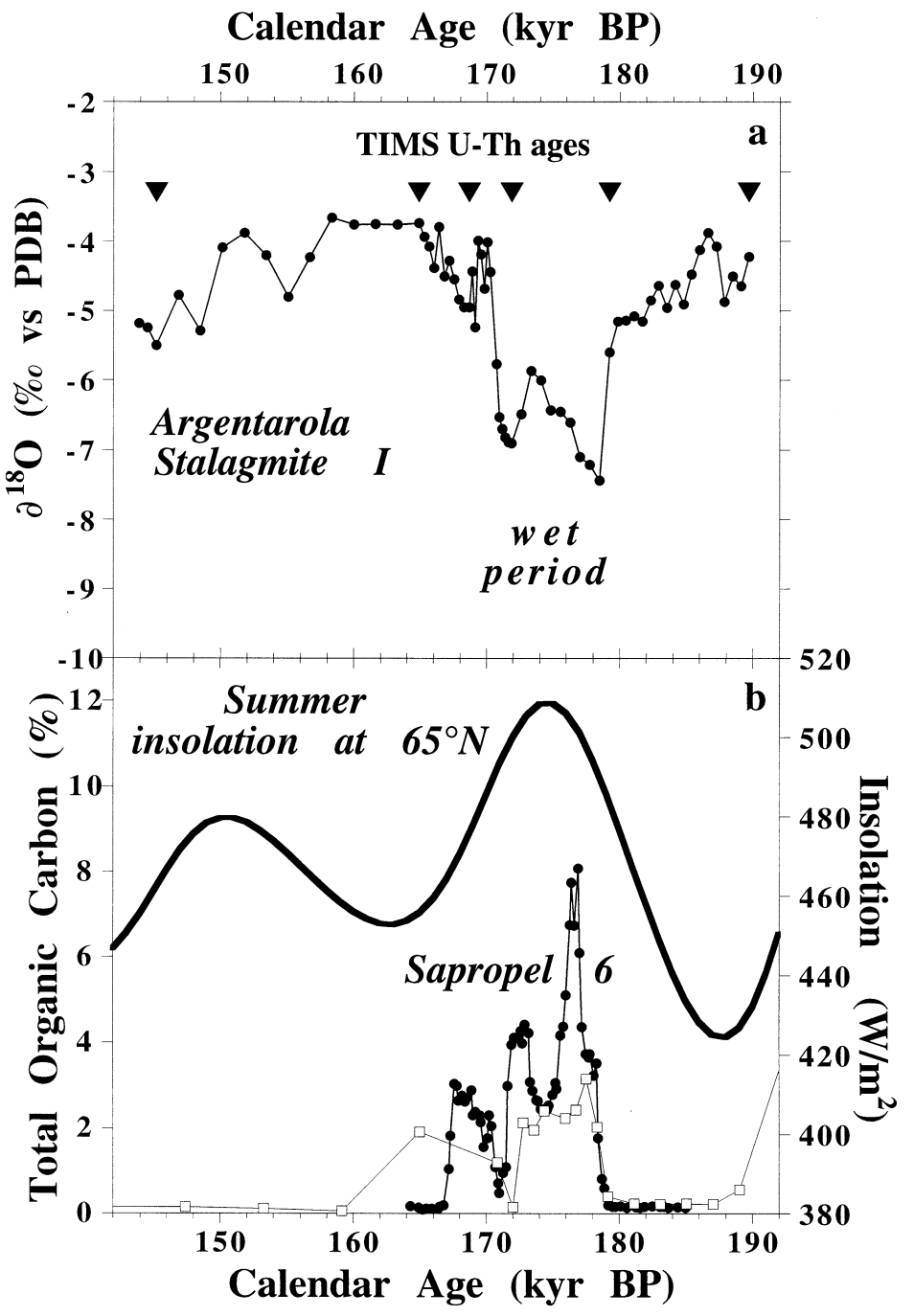

Fig. 8. (a) $\delta^{18}O$ plotted vs. calendar age for the Argentarola Cave stalagmite. Triangles show the age control points based on TIMS U–Th results. The 2σ error bars ranging between 1 and 2 kyr are smaller than the plotted symbols (see details in [32]). The period interpreted as humid occurred between 180 and 165 kyr BP. (b) The thick solid line shows the summer insolation at 65°N according to Laskar et al. [55], used by Lourens et al. [14] to synchronize sapropel events. The other records show the variations of TOC (in wt%) in two well-studied marine cores: open squares are for MD84641 [9,53] and black dots for KC19C (partly shown in [38]; updated TOC data from G.J. de Lange, pers. commun.).

tion (ca. 60% as calculated with the GCM results). Fig. 1a shows a recent $\delta^{18}O$ reconstruction for the global ocean [34] which amplitude for MIS 2 is compatible with $\delta^{18}O$ determinations in porewaters [35,36]. For MIS 6.5, the sea level scaled to the $\delta^{18}O$ record also agrees with a direct estimate of about 50 m below the present MSL [37]. In order to approximate the additional source effect, we calculated the difference between the $\delta^{18}O$ value for MIS 6.5 (ca. +0.4‰) and the average value for the two glacial substages MIS 6.6 (ca. +0.7‰) and 6.4 (ca. +1‰). The global ocean $\delta^{18}O$ during MIS 6.5 was thus about 0.5‰ lower when compared to MIS 6.6 and 6.4. This effect thus caused a further $\delta^{18}O$ depletion of the precipitation (60%×0.5‰ = 0.3‰) at our site.

All together, the $\delta^{18}O$ changes at the source of precipitation could range between 0.8‰ (0.5+0.3) and 1.5‰ (1.2+0.3). These changes remain significantly smaller than the 2–3‰ shift observed in the ASI stalagmite. This means that approximately 1–2‰ of the measured $\delta^{18}O$ decrease could be linked to the 'amount effect'. In Section 3 we determined its most probable slope at about 2‰ per 100 mm/month. This implies that rainfall during the isotopic excursion could have increased by 50–100 mm/month. This large range would be further widened to 25–200 mm/month by taking into account upper and lower bound values for the 'amount effect' (1 and 4‰ per 100 mm/month; see Table 1). This very large range illustrates the difficulty to quantify past rainfall from $\delta^{18}O$ measured in speleothems. Indeed, the largest changes are probably unlikely because the modern monthly precipitation is only 70 mm/month in the vicinity of Argentarola Island and 70 and 100 mm/month, respectively, for the east and west box of the GISS–GCM. Furthermore, it is interesting to note that the lower part of the range is compatible with the 40–50 mm/month increase simulated by the GISS–GCM model (175K–LGM difference for the east box which is most representative for our site; see Section 3). In any case, both amount and source effects are cumulative and, taken together, form the qualitative but clear $\delta^{18}O_p$ signature of a relatively humid episode during MIS 6.5, unusual under cold conditions.

5. Implications for paleoclimatic conditions during the sapropel 6 event

The U–Th ages for the inferred pluvial period fit well with other independent age determinations [14,38] for the sapropel 6 event (S6) which occurred during MIS 6.5. The two organic carbon records for S6 in Fig. 8b indicate that the humid event corresponds chronologically with the summer insolation maximum at 65°N centered at ca. 175 kyr BP. Insolation peaks linked to orbital precession variations are thought to be the primary forcing factor in the formation of sapropels in the Mediterranean Sea. These peaks are even used as chronological tuning targets to place sapropels on absolute time scales (e.g. [14,15,39,40]). Our work suggests there is little time lag between orbital forcing and the onset of pluvial conditions, which may even have started a few millennia earlier than the insolation maximum. The U–Th age for the end of the $\delta^{18}O$ anomaly is 165–170 kyr BP (Fig. 8a) which is compatible with recent Ar–Ar ages performed on volcanic layers located above S6 in marine sediments (161 ± 2 kyr BP for the W3 tephra [41] which originated from the Island of Kos).

The isotopic signature observed in ASI for the S6 event is similar to those observed in speleothems from the Soreq Cave in Israel [42,43]. These authors invoked pluvial conditions not only during the prominent interglacial sapropels (S1 and S5) but also for sapropels deposited during interstadials (S3 and S4) and even colder periods (S2, S6). The similarity between the $\delta^{18}O$ shifts as observed for S6 in Italy and S6, S4, S3 and S2 in Israel [42,43] clearly shows that both eastern and western Mediterranean basins experienced wetter conditions during these sapropel events.

These paleoclimatic conditions can be compared to those reconstructed from pollen counts in sapropel layers [40,44]. S6 is usually characterized by relatively high percentages of the genus *Artemisia* (sagebrush) and the Chenopodiaceae family and low percentages of the genus *Quercus* (oak). It is not easy to interpret the increased percentages on pollen diagrams because of the disappearance of trees (e.g. *Quercus*) during glacial periods (e.g. MIS 6) which leads to an auto-

matic increase of non-arboreal pollen percentages (e.g. *Artemisia* and Chenopodiaceae). Nevertheless, as explained by Ten Haven et al. [45], the steppic signatures observed for S6 could be linked to the widespread cooling which prevailed during the penultimate glaciation (e.g. relatively cold SSTs reconstructed with alkenones during the S6 event [15,33,45,46]). Although high abundances of *Artemisia* are found in dry conditions, species belonging to this genus may also be found in a variety of environments with annual precipitations ranging from 50 to 1100 mm/yr [47]. In any case, it is noteworthy that *Artemisia*, Chenopodiaceae and *Ephedra* percentages during S6 reported in [48] are broadly similar to those observed for other sapropel events interpreted as humid periods (e.g. S3, S4, S7 and S8).

Only a few long pollen sequences are available for southern Europe allowing to consider the paleoenvironmental conditions during the entire MIS 6. Tzedakis et al. [49] synchronized in detail the records of Valle di Castiglione (Italy), Ioannina and Tenaghi Philippon (both in Greece) and Bouchet–Praclaux (France). At each site there is subtle evidence for vegetation changes (e.g. increase of temperate trees) suggesting some climatic improvement during MIS 6.5 when compared to MIS 6.6 and 6.4. However, it is still difficult to disentangle the effects of drastic cooling from changes of moisture availability. Overall the vegetation distribution during MIS 6.5 is reminiscent of interstadial periods of the early part of MIS 3 (P.C. Tzedakis, pers. commun.).

The evidence for a relatively humid period in the Tyrrhenian Sea area during S6 suggests that this sapropel was caused mainly by a widespread increase in rainfall. Additional inputs of freshwater to the Mediterranean Sea may have come from rivers, both from fossil drainage systems in North Africa (e.g. [50]) and from melting continental ice during the transition between MIS 6.6 and 6.5. This sapropel event was accompanied by relatively cold temperatures as measured with alkenones [15,33,45,46] or planktonic foraminifera [9]. Since cooling favors ocean convection, the ocean stratification during S6 must have been almost entirely due to the salinity decrease caused by the dilution of ocean surface waters.

Notably, our results imply that surface ocean dilution probably occurred in the western Mediterranean basin and was thus not restricted to the Nile discharge area. This conclusion agrees not only with ocean studies [5,7,9,33] but also with a recent comparison between lacustrine and marine sequences from the central and western Mediterranean Sea [51]. One of the main conclusions by these authors is indeed that sapropel formation (S1 in their case) correlates with evidence in the terrestrial records for major increase in precipitation levels that affected the Italian mainland. Further confirmation comes from the study of discontinuous growth phases of a speleothem from the south of France [52].

Another interesting aspect of the stalagmite $\delta^{18}O$ record is that the negative anomaly corresponding to S6 is in fact rather complex, being composed of two minima at 178 and 172 kyr BP followed by a smaller event at 168 kyr BP (Fig. 8a). Isotopic data measured in stalagmites from Israel also indicate that several sapropels are characterized by multiple phases (e.g. S4, S3 and S3 in [42] and S6 in [43]). The isotopic signature observed for S6 in Israel closely resembles the one in Italy with a large and abrupt $\delta^{18}O$ depletion at ca. 180 kyr BP followed by smaller $\delta^{18}O$ minima [43]. Although it is difficult to separate the superimposed effects of precipitation amount and source composition on $\delta^{18}O$, we believe that these second-order structures are also linked to precipitation fluctuations. This is supported by the fact that most sapropel events exhibit multiple phases when studied at sufficient resolution in deep-sea sediments [8,11–13]. In particular, S6 is usually characterized by 2–3 peaks of total organic carbon (TOC) in the eastern Mediterranean [4,10,38,53]. Moreover, S6 is also present as a double TOC peak in cores from ODP site 975 [54] even if the TOC concentrations are typically low in the western Mediterranean basin. Fig. 8b presents the TOC record available for S6 in two deep-sea sediment cores with relatively high sedimentation rates and high TOC content (data for MD84641 are from [53]; data for KC19C kindly provided by G.J. de Lange were partly shown in [38]). The correspondence between the TOC maxima in core KC19C and

the $\delta^{18}O$ minima in the stalagmite is impressive especially because the chronologies of these records are completely independent (based on U–Th dating for ASI and on a linear interpolation between the S5 and S7 events which occurred during interglacial periods evidenced in core KC19C).

Besides the main $\delta^{18}O$ excursion corresponding to the S6 event, a smaller $\delta^{18}O$ anomaly is observed around 150 kyr BP which could be linked to the 150-kyr-BP insolation maximum (Fig. 8). No sapropel was deposited during that period but several authors described a relatively large $\delta^{18}O$ depletion in the eastern Mediterranean Sea during that time [33,43].

6. Conclusions

(1) In the Tyrrhenian Sea area, the period between 180 and 170 kyr BP was relatively wet compared with the rest of the penultimate glacial stage (MIS 6). This period is in phase with a summer insolation maximum at 65°N, which also corresponds to the deposition of sapropel 6 in the Mediterranean Sea.

(2) These results provide a further geochronological test on the direct influence of orbital variations on the hydrology of the mid to low latitudes zone.

(3) The complex fine structure of the stalagmite $\delta^{18}O$ record is also compatible with detailed studies performed on sapropels, further suggesting a direct link between pluvial conditions and Mediterranean sea surface stratification.

(4) The evidence for wetter conditions during S6 in the western Mediterranean basin agrees with several previous studies based on planktonic foraminifera and alkenones. Surface ocean dilution due to increased rainfall was probably not restricted to the Nile discharge area.

(5) The speleothem record suggests that pluvial conditions during S6 were similar to those during other sapropel events such as S4, S3 and S2. By contrast, more extreme hydrological conditions are associated with sapropel events (S5 and S1) when these took place during warm interglacial periods (MIS 5.5 and MIS 1).

Acknowledgements

We thank R. Cheddadi, K. Emeis, G.J. de Lange, L. Lourens, M. Rossignol-Strick, and C. Tzedakis for useful discussions, E. Goddard for technical assistance with stable isotopes, J.-J. Motte for help in producing Figs. 2 and 3, G.J. de Lange for providing TOC data from core KC19C, J. Ogg and two anonymous referees for reviews of the paper. Work at CEREGE was supported by CNRS (PNEDC) and the European Community (project STOPFEN). E.B. acknowledges NATO for a fellowship which supported his sabbatical stay at Harvard University.*[SK]*

References

[1] E.J. Rohling (Ed.), Fifth decade of Mediterranean paleoclimate and sapropel studies. Mar. Geol. 153 (1999) 1–347.
[2] M. Rossignol-Strick, W. Nesteroff, P. Olive, C. Vergnaud-Grazzini, After the deluge: Mediterranean stagnation and sapropel formation, Nature 295 (1982) 105–110.
[3] J.P. Sachs, D.J. Repeta, Oligotrophy and nitrogen fixation during Eastern Mediterranean sapropel events, Science 286 (1999) 2485–2488.
[4] M.B. Cita, C. Vergnaud-Grazzini, C. Robert, H. Chamley, N. Ciaranfi, S. D'Onofrio, Paleoclimatic record of a long deep sea core from the eastern Mediterranean, Quat. Res. 8 (1977) 205–235.
[5] R.C. Thunell, D.F. Williams, Glacial–Holocene salinity changes in the Mediterranean Sea: hydrographic and depositional effects, Nature 338 (1989) 493–496.
[6] J.L. Sarmiento, T. Herbert, J.R. Toggweiler, Mediterranean nutrient balance and episodes of anoxia, Glob. Biogeochem. Cycles 2 (1988) 427–444.
[7] K. Stratford, R.G. Williams, P.G. Myers, Impact of the circulation on sapropel formation in the eastern Mediterranean, Glob. Biogeochem. Cycles 14 (2000) 683–695.
[8] K.-C. Emeis, U. Struck, H.-M. Schulz, R. Rosenberg, S. Bernasconi, H. Erlenkeuser, T. Sakamoto, F. Martinez-Ruiz, Temperature and salinity variations of Mediterranean Sea surface waters over the last 16,000 years from records of planctonic stable isotopes and alkenone unsaturation ratios, Palaeogeogr. Palaeoclimatol. Palaeoecol. 158 (2000) 259–280.
[9] N. Kallel, J.-C. Duplessy, L. Labeyrie, M. Fontugne, M. Paterne, M. Montacer, Mediterranean pluvial periods and sapropel formation over the last 200,000 years, Palaeogeogr. Palaeoclimatol. Palaeoecol. 157 (2000) 45–58.
[10] B.J.H. van Os, J.J. Middelburg, G.J. de Lange, Possible diagenetic mobilization of barium in sapropelic sediment

from the eastern Mediterranean, Mar. Geol. 100 (1991) 125–136.
[11] J. Thomson, D. Mercone, G.J. de Lange, P.J.M. van Santvoort, Review of recent advances in the interpretation of eastern Mediterranean sapropel S1 from geochemical evidence, Mar. Geol. 153 (1999) 77–89.
[12] D. Mercone, J. Thomson, I.W. Croudace, G. Siani, M. Paterne, S. Troelstra, Duration of S1, the most recent sapropel in the eastern Mediterranean Sea, as indicated by accelerator mass spectrometry radiocarbon and geochemical evidence, Paleoceanography 15 (2000) 336–347.
[13] D. Mercone, J. Thomson, R.H. Abu-Zied, I.W. Croudace, E.J. Rohling, High-resolution geochemical and micropalaeontological profiling of the most recent eastern Mediterranean sapropel, Mar. Geol. 177 (2001) 25–44.
[14] L.J. Lourens, A. Antonarakou, F.J. Hilgen, A.A.M. Van Hoof, C. Vergnaud-Grazzini, W.J. Zachariasse, Evaluation of the Plio–Pleistocene astronomical timescale, Paleoceanography 11 (1996) 391–413.
[15] K.-C. Emeis, T. Sakamoto, R. Wehausen, H.-J. Brumsack, The sapropel record of the eastern Mediterranean Sea – results of Ocean Drilling Program Leg 160, Palaeogeogr. Palaeoclimatol. Palaeoecol. 158 (2000) 371–395.
[16] M.-A. Mélières, M. Rossignol-Strick, B. Malaizé, Relation between low latitude insolation and $\delta^{18}O$ change of atmospheric oxygen for the last 200 kyrs, as revealed by Mediterranean sapropels, Geophys. Res. Lett. 24 (1997) 1235–1238.
[17] V. Masson, P. Braconnot, J. Jouzel, N. de Noblet, R. Cheddadi, O. Marchal, Simulation of intense monsoons under glacial conditions, Geophys. Res. Lett. 27 (2000) 1747–1750.
[18] F. Antonioli, S. Silenzi, S. Frisia, Tyrrhenian Holocene palaeoclimate trends from spelean serpulids, Quat. Sci. Rev. 20 (2001) 1661–1670.
[19] G. Delmonaco, C. Margottini, A. Trocciola, Non stationarity of hydroclimatic data: the case study of the Tiber river basin, in: R. Casale, G.B. Pedroli, P. Samuels (Eds.), Ribamod-River basing modelling, management, flood mitigation: concerted action. Delft, 13–15 February, EUR 18019 EN, 1997, pp. 195–209.
[20] R.D. Koster, P.S. Eagleson, W.S. Broecker, Tracer water transport and subgrid precipitation variation within atmospheric general circulation models. Tech. Report 317, Ralph M. Parsons Laboratory, Department of Civil Engineering, Massachusetts Institute of Technology, Cambridge, MA, 1988.
[21] D. Pailler, E. Bard, High frequency paleoceanographic changes during the past 140, 000 years recorded by the organic matter in sediments off the Iberian Margin, Palaeogeogr. Palaeoclimatol. Palaeoecol. 181 (2002) 431–452.
[22] K. Rozanski, L. Araguas-Araguas, R. Gonfiantini, Relation between long-term trends of oxygen-18 isotope composition of precipitation and climate, Science 258 (1992) 981–984.
[23] K. Rozanski, L. Araguás-Araguás, R. Gonfiantini, Isotopic patterns in modern global precipitation, in: P.K. Swart, K.C. Lohmann, J. McKenzie, S. Savin (Eds.), Climate Change in Continental Isotopic Records. Geophysical Monograph 78, American Geophysical Union, Washington, DC, 1993, pp. 1–36.
[24] IAEA/WMO, Global Network for Isotopes in Precipitations. The GNIP Database, Release 3, October 1999. URL:http//isohis.iaea.org/.
[25] W. Dansgaard, Stable isotopes in precipitation, Tellus 16 (1964) 436–468.
[26] Mazor, E., Applied chemical and isotopic groundwater hydrology. Buckingham, Open University Press, 1991, 274 pp.
[27] J. Jouzel, G.L. Russell, R.J. Suozzo, R.D. Koster, J.W.C. White, W.S. Broecker, Simulations of the HDO and $H_2^{18}O$ atmospheric cycles using the NASA/GISS general circulation model: The seasonal cycle for present-day conditions, J. Geophys. Res. 92 (1987) 14739–14760.
[28] J.R. O'Neil, R.N. Clayton, T.K. Mayeda, Oxygen isotope fractionation in divalent metal carbonates, J. Chem. Phys. 31 (1969) 5547–5558.
[29] F. McDermott, D.P. Mattey, C. Hawkesworth, Centennial-scale Holocene climate variability revealed by a high-resolution speleothem $\delta^{18}O$ record from SW Ireland, Science 294 (2001) 1328–1331.
[30] C.H. Hendy, The isotopic geochemistry of speleothems – I. The calculation of the effects of different modes of formation on the isotopic composition of speleothems and their applicability as palaeoclimatic indicators, Geochim. Cosmochim. Acta 35 (1971) 801–824.
[31] J.M. Desmarchelier, A. Goede, L.K. Ayliffe, M.T. McCulloch, K. Moriarty, Stable isotope record and its palaeoenvironmental interpretation for a late Middle Pleistocene speleothem from Victoria Fossil Cave, Naracoorte, South Australia, Quat. Sci. Rev. 19 (2000) 763–774.
[32] E. Bard, F. Antonioli, S. Silenzi, Sea-level during the penultimate interglacial period based on a submerged stalagmite from Argentarola Cave (Italy), Earth Planet. Sci. Lett. 196 (2002) 135–146.
[33] K.-C. Emeis, H. Schulz, U. Struck, M. Rossignol-Strick, H. Erlenkeuser, M.W. Howell, D. Kroon, A. Mackensen, S. Ishizuka, T. Oba, T. Sakamoto, I. Koizumi, Eastern Mediterranean surface water temperatures and $\delta^{18}O$ composition during deposition of sapropels in the late Quaternary. Paleoceanography, in press.
[34] C. Waelbroeck, L. Labeyrie, E. Michel, J.C. Duplessy, J.F. McManus, K. Lambeck, E. Balbon, M. Labracherie, Sea-level and deep water temperature changes derived from benthic foraminifera isotopic records, Quat Sci. Rev. 21 (2002) 295–305.
[35] D.P. Schrag, G. Hampt, D.W. Murray, The temperature and oxygen isotopic composition of the glacial ocean, Science 272 (1996) 1930–1932.
[36] D.P. Schrag, J.F. Adkins, K. McIntyre, J. Alexander, D.A. Hodell, C. Charles, J. McManus, Reconstructing

the Oxygen Isotopic Composition of Seawater during the Last Glacial Maximum, Quat. Sci. Rev. 21 (2002) 331–342.

[37] P.L. Smart, D.A. Richards, R.L. Edwards, Uranium-series ages of speleothems from South Andros, Bahamas: Implications for Quaternary sea-level history and palaeoclimate, Cave Karst Sci. 25 (1998) 67–74.

[38] S. Severmann, J. Thomson, Investigation of the ingrowth of radioactive daughters of ^{238}U in Mediterranean sapropels as a potential dating tool, Chem. Geol. 150 (1998) 317–330.

[39] F.J. Hilgen, L. Lourens, A. Berger, M.F. Loutre, Evaluation of the astronomically calibrated time scale for the late Pliocene and earliest Pleistocene, Paleoceanography 8 (1993) 549–565.

[40] M. Rossignol-Strick, M. Paterne, A synthetic pollen record of the eastern Mediterranean sapropels of the last 1 Ma implications for the time-scale and formation of sapropels, Mar. Geol. 153 (1999) 221–237.

[41] P.E. Smith, D. York, Y. Chen, N.M. Evenson, Single crystal ^{40}Ar–^{39}Ar dating of a Late Quaternary paroxysm on Kos, Greece: Concordance of terrestrial and marine ages, Geophys. Res. Lett. 23 (1996) 3047–3050.

[42] M. Bar-Matthews, M.A. Ayalon, A. Kaufman, Timing and hydrological conditions of sapropel events in the eastern Mediterranean, as evident from speleothems, Soreq cave, Israel, Chem. Geol. 169 (2000) 145–156.

[43] A. Ayalon, M. Bar-Matthews, A. Kaufman, Climatic conditions during marine oxygen isotope stage 6 in the eastern Mediterranean region from the isotopic composition of speleothems of Soreq Cave, Israel, Geology 30 (2002) 303–306.

[44] G.M. Ganssen, S.R Troelstra, Paleoenvironmental change from stable isotopes in planktonic foraminifera from eastern Mediterranean sapropels, Mar. Geol. 75 (1987) 210–218.

[45] H.L. Ten Haven, M. Baas, M. Kroot, J.W. de Leeuw, P.A. Schenk, J. Ebbing, Late Quaternary Mediterranean sapropels III. Assessment of source of input and paleotemperature as derived from biological markers, Geochim. Cosmochim. Acta 51 (1987) 803–810.

[46] K.-C. Emeis, H.-M. Schulz, U. Struck, T. Sakamoto, H. Doose, H. Erlenkeuser, M. Howell, D. Kroon, M. Paterne, Stable isotope and alkenone temperature records of sapropels from sites 964 and 967: Constraining the physical environment of sapropel formation in the eastern Mediterranean Sea, in: A.H.F. Robertson, K.-C. Emeis, C. Richter, A. Camerlenghi (Eds.), Proc. ODP, Sci. Res. 160, 1998, pp. 309–331.

[47] D. Subally, P. Quézel, Glacial or interglacial *Artemisia*, a plant indicator with dual responses, Rev. Palaeobot. Palynol. 2443 (2002) 1–8.

[48] R. Cheddadi, M. Rossignol-Strick, Eastern Mediterranean Quaternary paleoclimates from pollen and isotope records of marine cores in the Nile cone area, Paleoceanography 10 (1995) 291–300.

[49] P.C. Tzedakis, V. Andrieu, J.L. de Beaulieu, H.J.B. Birks, S. Crowhurst, M. Follieri, H. Hooghiemstra, D. Magri, M. Reille, L. Sadori, N.J. Shackleton, T.A. Wijmstra, Establishing a terrestrial chronological framework as a basis for biostratigraphical comparisons, Quat. Sci. Rev. 20 (2001) 1583–1592.

[50] H.J. Pachur, S. Kröpelin, Wadi Howar: Paleoclimatic evidence from an extinct river system in the Southeastern Sahara, Science 237 (1987) 298–300.

[51] D. Ariztegui, A. Asioli, J.J. Lowe, F. Trincardi, L. Vigliotti, F. Tamburini, C. Chondrogianni, C.A. Accorsi, M. Bandini, A. Mazzanti, A.M. Mercuri, S. Van der Kaars, J.A. McKenzie, F. Oldfield, Palaeoclimate and the formation of sapropel S1: inferences from Late Quaternary lacustrine and marine sequences in the central Mediterranean region, Palaeogeogr. Palaeoclimatol. Palaeoecol. 158 (2000) 215–240.

[52] V. Plagnes, C. Causse, D. Genty, M. Paterne, D. Blamart, A discontinuous climatic record from 187 to 74 ka from a speleothem of the Clamouse cave (south of France), Earth Planet, Sci. Lett. 201 (2002) 87–103.

[53] M.R. Fontugne, S.E. Calvert, Late Pleistocene variability of the carbon isotopic composition of organic matter in the eastern Mediterranean: monitor of changes in carbon sources and atmospheric CO_2 concentrations, Paleoceanography 7 (1992) 1–20.

[54] L. Capotondi, L. Vigliotti, Magnetic and microfaunal characterization of Late Quaternary sediments from the western Mediterranean: interferences about sapropel formation and paleoceanographic implications, in: R. Zahn, M.C. Comas, A. Klaus (Eds.), Proc. ODP, Sci. Res. 161, 1999, pp. 505–518.

[55] J. Laskar, F. Joutel, F. Boudin, Orbital, precessional and insolation quantities for the Earth from −20 Myr to +10 Myr, Astron. Astrophys. 270 (1993) 522–533.